Thermal Control of Space X-Ray Experiment

R. L. Akau* and D. W. Larson‡
Sandia National Laboratories, Albuquerque, New Mexico

A thermal control system has been designed for the Uniformly Redundant Array (URA), which is a Shuttle-launched scientific experiment to detect and map x-ray sources in space. The URA thermal control system must ensure that the various components of the experiment survive and remain within operational temperature limits when exposed to temperature extremes of space resulting from different shuttle orientations. A thermal model was developed to simulate different orbital configurations; thermal-vacuum tests were conducted to test the reliability of the thermal hardware and verify the thermal model. The tests and analyses indicated that the thermal control system was able to meet the design goals.

Introduction

The Uniformly Redundant Array (URA) is a scientific experiment to detect and map x-ray sources in space. The detector incorporates a gas scintillator proportional counter (GSPC) and an imaging proportional counter (IPC) to provide improved energy and spatial resolution compared to previous conventional proportional counters in the energy range 0.1 to 60 ke V[1-4]. However, to obtain this resolution the temperature constraints are severe; the detector must be maintained to $\pm 1°C$ during use. A similar x-ray detector has been tested successfully over short periods of time during two sounding rocket launches.[5,6] Utilizing an x-ray detector over a longer-duration space flight would provide invaluable x-ray astronomy data. Therefore, the URA system was developed for operation from the cargo bay of the Space Shuttle and scheduled for a forthcoming launch.

A thermal control system has been developed for the URA experiment, and this paper presents the design procedure used, the development of the thermal models, and compares predicted and measured temperatures.

Description of URA Equipment

A schematic diagram of the URA experiment is shown in Fig. 1. The URA is attached to an experimental support structure (ESS) in the Shuttle bay along with several other experiments and will be operated by a payload specialist. It is mounted to the short-equipment section (SES) of the ESS as shown in Fig. 2 and is thermally isolated from any base-plate temperature control. The main components are the aperture, shroud, detector, digital electronics, power distribution box, and camera.

The aperture and detector are bolted to base-plates consisting of an inner layer of aluminum honeycomb covered on both sides with thin sheets of aluminum. The aperture base-plate is approximately 1.27 cm thick and the detector base-plate is 5.08 cm thick and tapers to 6.85 cm. The aperture consists of 15 hexagonal-shaped sheets of molybdenum (0.0152 cm thick) separated by spacers and held together with a structural "strong-back" that provides strength and support. The molybdenum sheets have a specified pattern of 25,000 hexagonal-shaped holes that must be carefully aligned to provide the required collimation of the incoming x-rays. The temperature gradients in the aperture must be minimized to reduce thermal stresses and prevent warping of the molybdenum sheets. Enclosing the aperture and detector is a shroud that is approximately 244 cm in length. The shroud consists of an aluminum honeycomb structure 1.27 cm thick covered with a thin aluminum sheet on the inner surface. The interior of the shroud

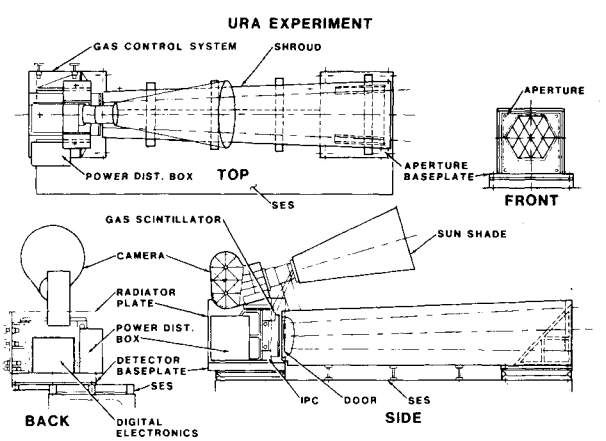

Fig. 1 Schematic diagram of URA experiment.

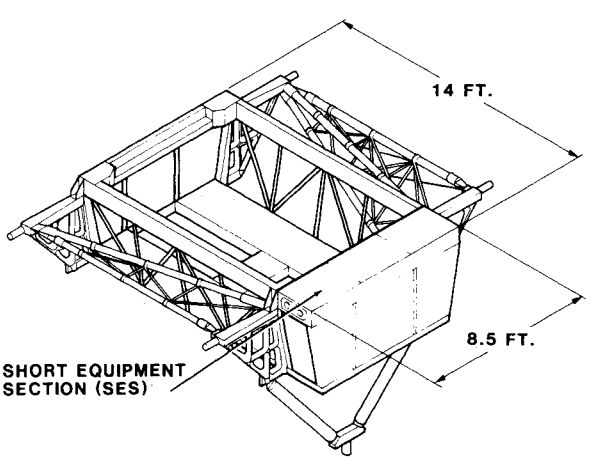

Fig. 2 Experimental support structure.

Presented as Paper 87-1572 at the AIAA 22nd Thermophysics Conference, Honolulu, HI, June 8-10, 1987; received June 25, 1987; revision received Jan. 20, 1989. This paper is declared a work of the U.S. Government and is not subject to copyright protection in the United States.

*Member Technical Staff, Fluid Mechanics and Heat Transfer Division III.

†Division Supervisor, Fluid Mechanics and Heat Transfer Division III.

walls are painted black. The outside surface of the shroud has a lead coating that is sufficient to stop 70 keV photons. The detector and aperture base-plates and the shroud are thermally isolated from the SES with a phenolic material that has a thermal resistance of 9.5°C/W. The aperture and detector base-plates and the shroud are not structurally connected to each other and have separate mounting points to the SES.

A long-time exposure camera, which is enclosed in an aluminum case, is attached to a platform above the detector and dissipates 2 W of internal heating. The camera tracks the orientation of the URA experiment relative to the stars when experimental data are being recorded and can operate from −54 to 70°C. However, the film can only survive a temperature range of −18 to 49°C. A conical-shaped sunshade 83 cm long is attached to the front of the camera case and is thermally isolated from the camera with a phenolic material.

The URA detector is made of aluminum and consists of gas scintillator and imaging proportional counters (GSPC and IPC). During use it must be controlled to ±1°C. The nominal operating temperature is 40°C; however, it can function up to 45°C as long as the temperature variation is minimal while taking data. In addition, the detector is limited to a temperature change of less than 15°C per hour to ensure survival when not in use. The detector dissipates a total of 13 W of internal heat when operating. A "getter" located in the front of the detector generates 25 W of power when in operation. The operating time of the getter during flight will depend on the amount of gas purification needed in the GSPC and IPC. The detector, which is electrically isolated from the detector base-plate, is suspended above the detector base-plate by two aluminum frames attached to each side of the detector.

Located in back of the URA detector are the digital electronics box (EBOX) and the power distribution box (PDB), each of which dissipate 45 W when the URA system is powered on. The EBOX consists of module boards that are attached to a mother board and enclosed in an aluminum case. The PDB is cantilevered to one side of the detector and consists of a module box (5 W internal heating) and low-voltage power supply (40 W of internal heating) attached to an aluminum base-plate and enclosed by an aluminum cover. The temperature limits for the PDB and EBOX electronics range from −10 to 70°C.

Thermal Model

To ensure that the URA experiment will interface with other systems scheduled for the same Shuttle flight and will not adversely affect thermal control of adjacent experiments, several requirements must be met. These include:

1) Use a maximum of 135 W of auxiliary heating power.

2) Maintain the URA interface temperature at the contact with the SES mount brackets between −17.8 and 37.8°C.

3) Provide a simplified thermal model of the URA that could be integrated into a thermal systems model of the cargo bay.

4) Ensure the survival of the experiment when exposed to various orbital and Shuttle orientations and specify orbital conditions that require the experiment to be shut down to prevent overheating.

To provide design guidance, thermal models of the early URA configuration were developed using the thermal analyzer code SINDA.[7] These models were used to investigate the effects of heater capacity and location, thermal control surface conditions including metallized selective surfaces and multilayer insulation (MLI), and the temperature of other surfaces in the Shuttle bay. Steady-state temperatures were calculated from these early thermal models for the extreme conditions of full sun in the bay (hot) and with the cargo bay facing space with no solar heating (cold). These early models were then reduced to a highly simplified but representative 20-node model of the URA external configuration that was integrated into the STS SPORTS[8] thermal model, which simulates the thermal response of the Orbiter midsection during prelaunch, ascent, orbit, entry, and postlanding.

Subsequent to the development of these early thermal models, a number of design changes were made to the URA. One of the major changes was to relocate the PDB box from the top of the shroud to its current site on the side of the detector (see Fig. 1). To account for these modifications and provide information on the transient thermal response of the URA, a more detailed thermal model that permitted simulation of the time-varying thermal environment during orbit was developed using SINDA. The model consisted of 144 nodal points (including boundary temperatures of Earth and space). The nodes for the shroud and aperture, camera and sunshade, PDB, EBOX, and radiator plate and gas system panel are illustrated in Figs. 3–7. Included in the model are conductive and radiative heat transfer, wavelength-dependent radiative properties, orbital solar, albedo, and earthshine heat fluxes, internal heat sources due to thermal dissipation from electrical equipment, and thermostatically controlled resistance heaters. For this misssion, the Shuttle is scheduled to operate in a circular orbit at 150 n.mi. and at different β angles as shown in Fig. 8, where β is the angle between the sun vector and the orbit plane.

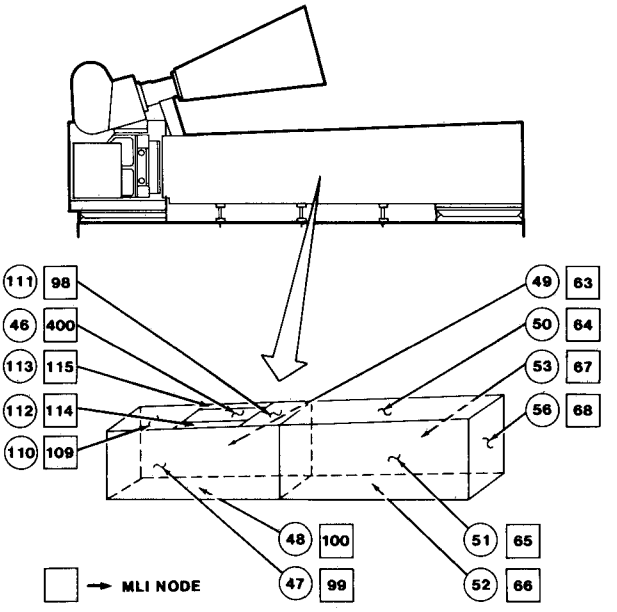

Fig. 3 Thermal model nodes for shroud and aperture.

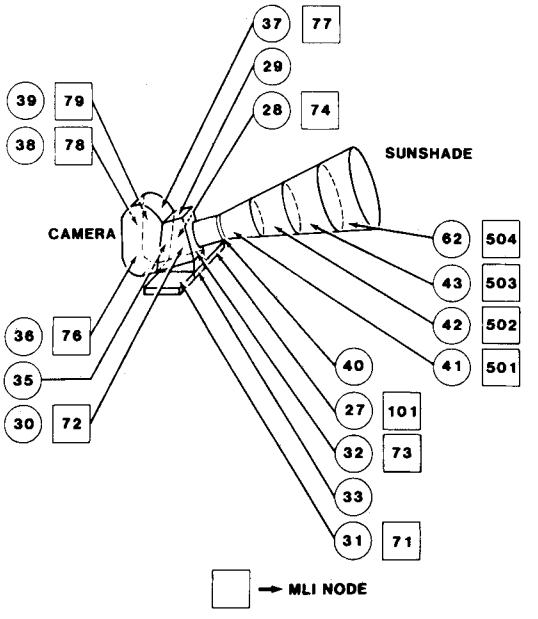

Fig. 4 Thermal model nodes for camera and sunshade.

Thermal Control Hardware

Because the URA must be thermally isolated from the SES, thermal control devices such as strip heaters, thermostats, and selective surface materials (wavelength-dependent radiative properties) are needed to maintain the experiment within the required temperature limits during extreme conditions. The 135 W of heater power for the URA experiment were distributed, as shown in Table 1. The electrical resistive heaters are thin, flexible, etched-foil heating elements, insulated with Kapton, and have a pressure-sensitive adhesive for easy application. The thermostats are bimetallic devices that are hermetically sealed. A single calibrated thermostat is aligned in series with each heater. The detector temperature is monitored with a thermistor that controls the detector heaters to $\pm 1°C$ with digital electronics. However, as a safety precaution, the detector heaters also include in-line thermostats that are designed to remain closed below $57.2 \pm 1.7°C$ and open 1-3°C above the closing temperature. Temperature control for the other parts of the URA is provided by the thermostats that are designed to remain closed below $10 \pm 2°C$ and open 1-3°C above the closing temperature. All the thermostats are designed to remain open on temperature rise.

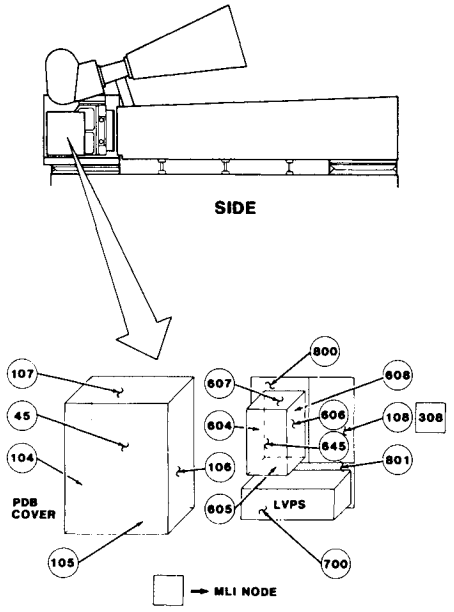

Fig. 5 Thermal model nodes for PDB.

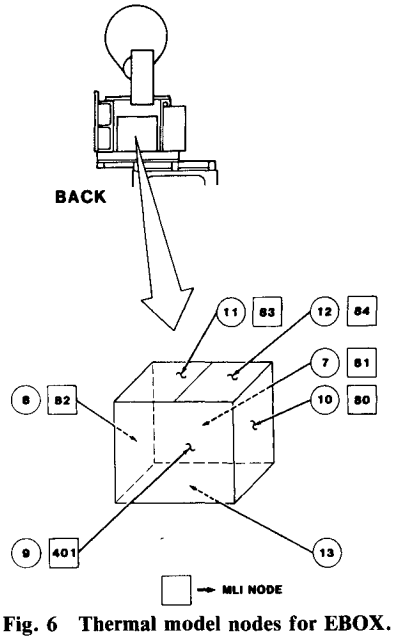

Fig. 6 Thermal model nodes for EBOX.

To assist in maintaining proper thermal control for the critical parts of the URA, thin sheets of metalized film with selective surfaces are used at various locations. The selective surface properties provide for thermal control by permitting the specifications of a wide range of the ratio α_s/ϵ_i, where α_s is the solar absorptivity and ϵ_i is the infrared emissivity. These materials either have selective surfaces on both sides or selective surface on one side and an adhesive on the other to attach to other surfaces. MLI, which also has selective surface properties, consists of thin layers of metallized film separated by an intervening netting and is used to minimize radiation heat loss and insulate the shroud, detector, camera, and the bottom of the detector and aperture base-plates.

The MLI blanket contains eight layers of double-sided metallized film. Each of the six inside layers of the MLI consists of 0.3-mil-thick aluminized Kapton. The layers are perforated for venting during ascent. The solar absorptivity and

Table 1 Heater locations on URA experiment

Location	No. of heaters	Power per heater, W	Total power, W
Aperture	3	5	15
Camera	3	5	15
Detector	6	5	30
Gas-control system	4	5	20
EBOX	3	15	45
PDB	2	5	10

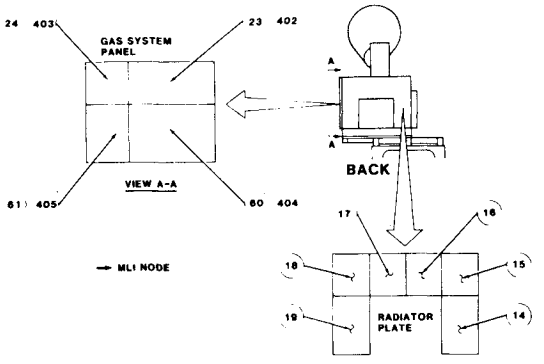

Fig. 7 Thermal model nodes for radiator plate and gas-system panel.

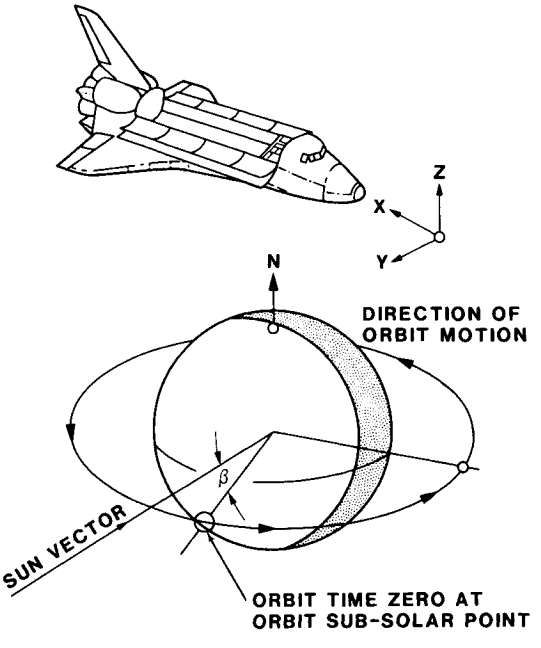

Fig. 8 Orbital orientation of Shuttle.

infrared emissivity values for this material are $\alpha_s \leq 0.14$ and $\epsilon_i \leq 0.05$. The aluminized Kapton material can survive temperature extremes from -251 to 288°C without degradation. The inside and outside layers of the MLI blanket are a bonded composite of 0.25-mil Mylar, aluminized on one side, Dacron netting, and a 0.5-mil Mylar layer aluminized on one side. The Dacron netting gives added strength to the material. The radiation surface properties for both sides of the material are $\alpha_s \leq 0.14$ and $\epsilon_i \leq 0.08$. This material is porolated (13,000 holes per square foot) for venting with holes that are barely visible. The continuous temperature range for this material is -184 to 107°C. A 100% polyester netting is placed between each layer to minimize conduction heat transfer.

Two types of selective surface adhesive tapes were used. They included 1.0-mil aluminized Kapton tape ($\alpha_s = 0.10$, $\epsilon_i = 0.02$) to minimize heat loss from the PDB cover, and a 5.0-mil aluminized Teflon tape ($\alpha_s = 0.14$, $\epsilon_i = 0.81$) used on the radiator plate, top side of the camera cover, and the top cover of the power distribution box to enhance the radiative heat loss and reduce the temperatures resulting from the internal dissipation of these components. Two layers of metallized film were placed over the EBOX to serve as a radiator. This material is aluminized on one side ($\alpha_s = 0.12$. $\epsilon_i \leq 0.07$) on 0.5-mil Kapton ($\alpha_s = 0.5$, $\epsilon_i = 0.8$) and survives temperatures from $-184°$ to 204°C. The selective surface adhesive tapes could not be placed on the outer surface of the EBOX because of its irregular surface. A single layer of metallized material is used to cover the outer surface of the aperture, since the metallized film would absorb the incoming x-rays if multiple layers were used. This single layer provided adequate thermal insulation to prevent large temperature gradients in the aperture, whereas the metallized film (both sides) was thin enough to allow the x-rays to pass.

Thermal-Vacuum Tests

Thermal-vacuum tests were conducted in a 7ft-diam vacuum chamber to check the operation of the thermal control system and to validate the thermal model. The inner wall of the vacuum chamber (shroud) is cooled or heated with liquid nitrogen and rod heaters. Because of the size limitation of the vacuum chamber, the aperture, sunshade, and shroud were not included in the tests. These tests essentially simulate a cold orbital condition with no solar or albedo heat fluxes.

The system was mounted to a base-plate that could be heated or cooled to a desired temperature. The detector and camera were covered with the MLI. The gas-mounting plate and EBOX were covered with single- and two-layer metallized material, respectively. MLI was not placed between the URA base-plate and the heating and/or cooling base-plate for this test. However, during the actual flight MLI will be placed below the base-plate to isolate the URA from the SES. Since the shroud and aperture were not included in the tests, the front of the detector was also covered with MLI. Two thermal balance tests were conducted with the average vacuum chamber wall temperatures at -73.9 and -21.1°C for the cold and hot tests, respectively. The average base-plate temperatures for the two tests were approximately 5.3 and 15°C, respectively.

A total of 22 copper-constantan thermocouples were placed at different locations on the URA to record time-temperature data. The thermocouples located on the URA are shown in Fig. 9. Six thermocouples were placed on the inner wall of the vacuum chamber. The temperatures were recorded until steady-state temperatures were obtained for each test. The URA system also has internal temperature monitors (thermistors), also shown in Fig. 9, which were recorded on a separate data acquisition system.

Table 2 Comparison of thermocouple and thermistor temperatures

	Temperature, °C	
Location	Thermistor	Thermocouple
Camera:		
Cold test	6.0	13.3
Hot test	8.0	15.0
Detector:		
Cold test	41.2	45.0
Hot test	46.0	46.7
EBOX:		
Cold test	19.0	19.4
Hot test	32.0	29.7
PDB base-plate:		
Cold test	20.1	21.1
Hot test	31.0	31.9
Gas-control system:		
Cold test	4.0	− 8.9
Hot test	2.0	− 1.1

Table 3 Comparison of measured and predicted steady-state results

		Temperature, °C			
		Cold test		Hot test	
Thermocouple number	Model node no.	Thermocouple	Model	Thermocouple	Model
Camera:					
1	30	12.8	14.7	13.9	16.4
2	32	15.0	13.2	15.0	15.9
Detector:					
3	2	46.1	44.4	47.2	44.7
4[a]	3,4		44.6		44.8
5	4	43.9	44.6	46.1	45.3
6	5,6	45.0	45.1	45.0	45.3
PDB:					
7	801	22.2	31.4	32.8	42.9
8	108	20.0	27.6	31.1	39.3
9	45	− 2.2	1.4	16.1	19.3
17[b]	700	31.7	32.0	43.3	45.0
LBOX:					
10	7	17.8	22.1	27.2	26.3
11	11,12	15.6	15.7	26.7	21.7
12	9	− 10.0	6.1	7.2	14.1
Radiator plate:					
13	15,18	− 20.0	− 2.3	2.2	9.8
Gas-control system:					
14	61	− 8.9	12.7	− 1.1	14.9

[a]Thermocouple 4 malfunctioned during tests. [b]Temperature monitor is a thermistor.

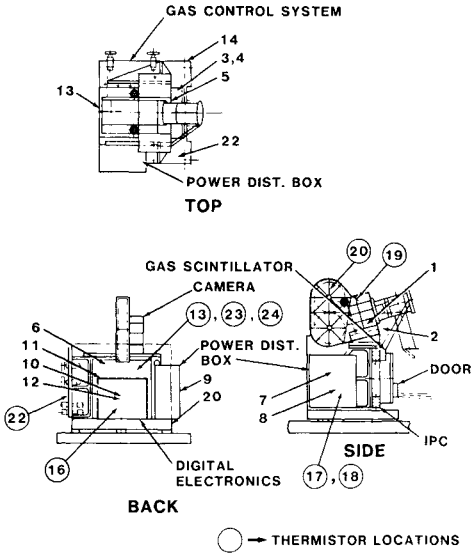

Fig. 9 Thermocouple and thermistor locations for thermal-vacuum test.

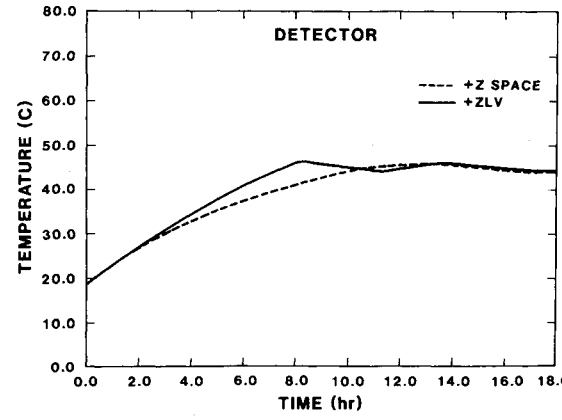

Fig. 10 Comparison of average predicted detector temperatures for +ZLV and +Z space orbits.

Discussion of Thermal-Vacuum Results

Table 2 shows a comparison of the thermistor and thermocouple steady-state temperatures at different locations of the URA system. The different temperature measuring systems compared reasonably well except for the camera section where the thermistor temperatures were 7°C lower than the thermocouples. The results in Table 2 also illustrate that the detector and camera thermocouple temperatures did not change apreciably during the transition from the cold to the hot test due to the effectiveness of the MLI.

A comparison of temperatures measured by the thermocouples and predicted by the thermal model is given in Table 3. The calculated results in Table 3 are for a low-voltage power supply (LVPS) internal heating of 20 W. Initially, it was anticipated that this power supply would produce 40 W of internal power. However, during the tests, power measurements indicated that only about 20 W were being dissipated. When the original 40 W were used in the model, the PDB temperatures were over 40°C higher than the measured temperatures. With the correct internal heating rate the model temperatures were 7°C higher for the PDB base-plate (thermocouples 7 and 8), but the PDB cover temperature (thermocouple 9) compared very well. The LVPS temperatures from the model (node 700) were 31.7 and 43.3°C, and the thermistor (no. 17) recorded 32.0 and 45.0 for the hot and cold tests, respectively.

The measured radiator plate temperatures were approximately 18 and 7°C lower for the cold and hot tests than the model predictions. This could be due to poor thermal contact between the radiator plate and EBOX. The gas-control system temperatures were 21 and 16°C lower for the cold and hot tests, respectively, than the model predicted. This was attributed to the thermal blanket not completely covering the gas panel (i.e., gaps and openings).

During the tests, the getter on the detector was turned on for 4.5 h and the temperatures for thermocouples 3, 5, and 6 increased 5°C. Therefore, the average change in temperature during the transition was 1.1°C per hour. The effect of getter thermal dissipation was also implemented into the thermal model, and a change of 1.7°C per hour was calculated. Since the getter is not controlled by the thermal control system but functions as needed to purify the gas in the GSPC and IPC, the detector temperature will need to be monitored by the payload specialist whenever the getter is on to prevent overheating of the detector.

The URA detector is designed to have 30 W of heater power. However, during thermal-vacuum tests, only 25 W of heater power were used on the detector. The detector temperature increased from an initial temperature of 18 to 45°C at a rate of 3°C per hour as compared to a prediction of 2°C per hour from the model with 25 W of detector heater power. Thus, while in flight (assuming 25 W of heater power to be conservative), the measured detector temperatures indicate that detector heaters will need to be on for at least 8 h (12.5 h from the model) before tests can be conducted at a detector temperature of 45°C if the initial temperature is 20°C. Tests were also performed to verify that all of the thermostats were operating at their prescribed set points.

Calculated URA Temperatures

Since the thermal-vacuum tests indicated that the detailed URA thermal model predicts temperatures reasonably well, the model was used to predict the system temperatures for extreme operating orbital conditions. A thermal design report[9] specified that the hottest and coldest operating environments were, respectively, 1) +ZLV orbit, when cargo bay has a maximum heat load (facing Earth with albedo and earthshine at $\beta = 0$), and 2) when the cargo bay is looking at space with no solar heat flux, at +Z space.

The thermal model assumes that when the cargo bay faces space there is no albedo and earthshine on the URA, and when the cargo bay faces Earth there are only albedo and earthshine external heat fluxes. URA temperatures were calculated until quasi-steady-state conditions were achieved. Table 4 shows the maximum and minimum temperatures for the extreme operating conditions and the overall maximum and minimum temperatures. The results are for a detector operating temperature of 45 ± 1°C and 30 W of detector heater power.

The results in Table 4 show that the detector operated at 44.9 ± 1.5°C, which is above the required temperature constraint of ± 1°C. However, the ± 1.5°C temperature variation is realistic and will not degrade the accuracy of the detector measurements. For the +Z space orbit, 12 h were required to heat the detector (30-W heater power) from 18 to 45°C, and only 8 h were required for the +ZLV orbit. A comparison of the detector temperature response for the two orbits is illustrated in Fig. 10. The overall predicted maximum and minimum temperatures from Table 4 and the required operational temperature limits are shown in Table 5. The maximum and minimum temperatures for the EBOX (39.3 and 1.1°C) and the PDB low-voltage power supply (45.2 and 21.3°C) were well within the desired operating temperature range of −10 to 70°C. Also, the camera maximum and minimum calculated temperatures were 23.7 and −4.8°C, respectively; the film cartridge temperature range was 17.1 to 6.3°C. The desired operating temperature range is −54 to 70°C for the camera and −18 to 49°C for the camera film. The thermal interface between the URA contact points to the SES mount brackets ranged from −0.3 to 36.6°C (detector and aperture base-

Table 4 Maximum and minimum predicted temperatures for extreme operating conditions

	Temperature, °C					
	+ Z space		+ ZLV		Overall	
Location	Maximum	Minimum	Maximum	Minimum	Maximum	Minimum
Detector	45.9	44.8	46.4	43.4	46.4	43.4
EBOX	19.4	1.1	39.3	24.8	39.3	1.1
PDB LVPS	21.3	21.3	45.2	45.2	45.2	21.3
Aperture	10.2	10.2	19.2	19.2	19.2	10.2
Shroud	15.6	9.4	25.3	21.4	25.3	9.4
Camera	15.1	− 4.8	23.7	12.0	23.7	− 4.8
Film cartridge	9.4	6.3	17.1	15.9	17.1	6.3
Aperture base-plate	2.3	− 0.3	24.7	19.8	24.7	− 0.3
Detector base-plate	25.2	3.3	36.3	25.1	36.3	3.3

Table 5 Comparison of predicted overall extreme temperatures and operational temperature limits

	Temperature, °C			
	Predicted		Design	
Location	Maximum	Minimum	Maximum	Minimum
Detector	46.4	43.4	46.0	44.0
EBOX	39.3	1.1	70.0	− 10.0
PDB LVPS	45.2	21.3	70.0	− 10.0
Camera	23.7	− 4.8	70.0	− 54.0
Film cartridge	17.1	6.3	49	− 18.0
Detector and aperture baseplates	36.6	− 0.3	37.8	− 17.8

plates), which falls within the specified constraints of − 17.8 and 37.8°C.

It is anticipated that the URA will not operate during orbital configurations that result in full sun in the cargo bay. Nevertheless, temperatures were calculated for this orbital configuration to determine if the system could operate in such a condition and to assure that the maximum expected temperatures did not exceed survivable (nonoperational) limits. The detector heating rate from 18 to 45°C was approximately the same as that predicted for the + ZLV orbit condition (3.4°C per hour). The predicted temperatures for most locations on the system during full sun were generally lower than temperatures calculated for the + ZLV orbit. However, the shroud and aperture temperatures continued to increase after 12 h, which caused the detector to go above its desired operating temperature, but not above survivable conditions. Therefore, the URA experiment could be operated during the early portions of a full-sun configuration, but could not be operated continuously in that condition.

Conclusions

The testing and analyses of the URA control system indicate that all of the components will remain within operational temperature limits when in use and within survivable limits when not in use. Furthermore, the thermal interface requirements with the spacecraft can be met. However, the desired operational temperature constraint of ± 1°C on the detector appears to exceed the capabilities of this system. Temperature variations of ± 1.5°C at the detector appear to be realistic and will provide for reasonable accuracy for the detector measurements. In addition, since the overall limitation of available heater power leads to an allocation of 30 W for the detector, the thermal mass associated with the detector can be heated only at approximately 3.4°C per hour. Therefore, several (8–12) hours will be required to heat the detector from initial ambient conditions to operational conditions. Also, once the detector is at temperature, if the getter is operating it will produce a detector temperature change of 1.1 to 1.7°C per hour. Since the getter functions independently from the thermal control system, the detector temperature will need to be monitored by the payload specialist whenever the getter is in operation to prevent the detector from overheating.

Acknowledgments

This work was performed at Sandia National Laboratories, supported by the U.S. Department of Energy under Contract DE-AC04-76DP00789.

Many individuals have been involved in developing the URA system. Some of these who helped in developing the thermal control system include Sandians G. Peterson and K. Scurry (mechanical design of the EBOX and LBOX), J. Chavez, B. Pershall, J. Klarkowsky, and J. Turner (electrical design of the EBOX and PDB and software development of the temperature control program), J. Freshour and R. Goekler (thermal-vacuum test support), and H. Lucero and L. Whinery of the Parachute Lab (fabrication of the MLI). In addition, we were assisted by E. Fenimore, D. Roussel-Dupre, and K. Christensen of Los Alamos National Laboratories, and W. Ku and I. Rochwarger of Columbia University.

References

[1]Hamilton, T. T., Hailey, C. J., Ku, W. H. M., and Novick, R., "A High Resolution Gas Scintillation Proportional Counter for Studying Low Energy Cosmic X-Ray Source," *IEEE Transactions on Nuclear Science,* Vol. NS-27, No. 1, Feb. 1980, pp. 190–195.

[2]Ku, W. H. M. and Hailey, C. J., "Properties of an Imagining Gas Scintillation Proportional Counter," *IEEE Transactions on Nuclear Science,* Vol. NS-28, No. 1, Feb., 1981, pp. 830–834.

[3]Hailey, C. J., Ku, W. H. M., and Vartanian, M. H., "An Imaging Gas Scintillation Proporational Counter for Use in X-Ray Astronomy," *Nuclear Instruments and Methods,* Vol. 213, 1983, pp. 397–410.

[4]Ku, W. H. M., Lum, K. S., and Vartanian, M. H., "A Large Area Imaging Gas Scintillation Proportional Counter for Use In X-Ray Astronomy," *Proceedings of the SPIE Conference on Instrumentation in Astronomy,"* Vol. 445, International Society for Optical Engineering, London, 1983, pp. 384–393.

[5]Vartanian, M. H., Lum, K. S., and Ku, W. H. M., "Imaging X-Ray Spectrophotometric Observation of SN 1005," *The Astrophysical Journal,* Vol. 288, 1985, pp. L5–L9.

[6]Reid, P. B., Ku, W. H. M., Long, K. S., Novick, R., and Pisarski, R. L., "A Drift Multiwire Proportional Counter for Cosmic Soft X-Ray Imaging," *IEEE Transactions on Nuclear Science,* Vol. NS-25, No. 1, 1979.

[7]Smith, J. P., "System Improved Differencing Analyzer (SINDA) User's Manual," TRW Systems Group, Redondo Beach, CA, April 1971.

[8]"Simplified Payload/Orbiter Simulator (SPORTS Model)," U.S. Air Force Space Division, El Segundo, CA, SD-YV-0065, April 1981.

[9]Crotty, D. A., "Thermal Design Requirements, Air Force Program 675," Lockheed Missiles & Space Company, Sunnyvale, CA, March 1984.